AD________________

Award Number: W81XWH-06-1-0620

TITLE: Multifunctional nanocomposites for Breast Cancer Imaging and Therapy

PRINCIPAL INVESTIGATOR: Swapan K. Gayen,Ph.D.
Valeria Balogh-Nair, Ph. D.

CONTRACTING ORGANIZATION:

Research Foundation of CUNY
New York, NY 10031

REPORT DATE: July 2008

TYPE OF REPORT: Final

PREPARED FOR: U.S. Army Medical Research Materiel Command
Fort Detrick, Maryland 21702-5012

DISTRIBUTION STATEMENT:

Approved for public release; distribution unlimited

REPORT DOCUMENTATION PAGE

Form Approved OMB No. 0704-0188

1. REPORT DATE *(DD-MM-YYYY)*
01-07-2008

2. REPORT TYPE
Final

3. DATES COVERED *(From - To)*
10 Jul 2006 – 09 Jun 2008

4. TITLE AND SUBTITLE
Multifunctional nanocomposites for Breast Cancer Imaging and Therapy

5a. CONTRACT NUMBER

5b. GRANT NUMBER
W81XWH-06-1-0620

5c. PROGRAM ELEMENT NUMBER

6. AUTHOR(S)
Gayen, S. K., Balogh-Nair, V

5d. PROJECT NUMBER

5e. TASK NUMBER

5f. WORK UNIT NUMBER

7. PERFORMING ORGANIZATION NAME(S) AND ADDRESS(ES)
Research Foundation of CUNY

New York, NY 10031
E-mail: rmaster@sci.ccny.cuny.edu

8. PERFORMING ORGANIZATION REPORT NUMBER

9. SPONSORING / MONITORING AGENCY NAME(S) AND ADDRESS(ES)

US Army Medical Research and Materiel Command

Fort Detrick, MD 21702-5012

10. SPONSOR/MONITOR'S ACRONYM(S)
USAMRAA

11. SPONSOR/MONITOR'S REPORT NUMBER(S)

12. DISTRIBUTION / AVAILABILITY STATEMENT

Approved for public release; Distribution unlimited

13. SUPPLEMENTARY NOTES

14. ABSTRACT

The objective of the research was to explore the feasibility of concomitant detection and therapy of breast cancer through the development of multifunctional nanocomposites that will enable early detection of breast tumors, visualization of dormant metastatic cells and prevent their spread. Fluorescent nanocomposites consisting of CdS and PbS quantum dots (QDs) encapsulated in dendrimers, a class of organic macromolecules, were synthesized, and their optical absorption spectra, emission spectra, and fluorescence lifetime were measured. The CdS-based nanocomposites fluoresced in the visible, and PbS-based nanocomposites fluoresced in the near-infrared spectral regions. Optical imaging experiments demonstrated the potential for using these nanocomposites as contrast agents. Three chemokine mimics were synthesized and a toxicity study carried out under a collaborative arrangement showed that none of the mimics to be toxic to MDA MB 468 breast cancer cell lines. Attempts were made to conjugate a chemokine to PbS-dendrimer nanocomposite surface.

15. SUBJECT TERMS
Breast cancer, multifunctional nanocomposite, semiconductor quantum dots, dendrimers, chemokines, contrast agents, near-infrared imaging, fluorescence imaging

16. SECURITY CLASSIFICATION OF: a. REPORT	b. ABSTRACT	c. THIS PAGE	17. LIMITATION OF ABSTRACT	18. NUMBER OF PAGES	19a. NAME OF RESPONSIBLE PERSON
Unclassified	Unclassified	Unclassified	Unclassified	17	USAMRMC
					19b. TELEPHONE NUMBER *(include area code)*

Table of Contents

Page

4. INTRODUCTION

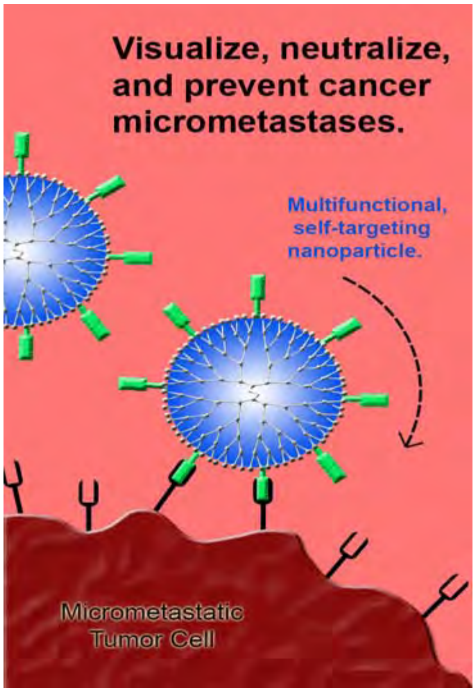

Figure 1. Self-targeting QDs against cancer

It is well known that breast cancer metastases are responsible for relapse and mortality, and that they show an organ-specific pattern of spread. It is also known that chemokine receptors CXCR4 and CCR7 are upregulated in breast cancer cells and in their micrometastases, and that the chemokine ligands for these same receptors are found at elevated levels in the areas to which breast cancer metastasizes. However, recent advances in our understanding of the disease in molecular terms have not yet triggered radical changes in breast cancer therapy because they do not deal with detection cum prevention of micrometastases; this work does. The purpose of the research was to test the feasibility of an approach, that unlike any therapy now in use, was designed to detect and prevent formation of micrometastases by blocking the CXCR4 receptor's interaction with its natural ligands using multivalent[1] synthetic chemokine mimics. The noninvasive NIR imaging method will image breast tumor and cancer micrometastases thereby eliminating surgical trauma. The dendrimer-based, biocompatible nontoxic nanoparticles that were synthesized in water, when loaded with multiple copies of the non-toxic VBN-chemokine mimics will not only allow visualization of micrometastases, but will also prevent their spread to other organs thereby changing the fatal outcome of the disease.

5. BODY

Specific Aim 1. Synthesize dendrimer-encapsulated QDs that absorb and emit efficiently in the NIR.

Task 1. Synthesize fifth generation surface modified 5G-PAMAM-dendrimer encapsulated PbS and InP QDs (0-4 months) and Task 2. Measure the absorption, fluorescence and excitaion spectra of the above synthesized dendrimer nanocomposite (1-4 months)

Syntheses of PbS QDs, using "top-down" or "bottom-up" protocols described in the literature[1] could not be adapted to prepare the target compounds, because of the low stability of the thiolate-capped PbS QDs at physiological pH values. The following approach, consisting of 3 phases, was pursued and ultimately led to the synthesis of stable, high quality, dendrimer-encapsulated PbS QDs:

In Phase 1, model reactions were run to obtain PAMAM dendrimer-encapsulated CdS QDs in an organic solvent (methanol) to determine the most suitable dendrimer generation size and other reaction conditions. In Phase 2, biocompatible synthesis in ultrapure, 18.2 MΩ water of CdS QDs within G5- and G6-PAMOH dendrimer nanoreactors was established, and in Phase 3, successful synthesis of stable, dendrimer-encapsulated PbS QDs was achieved via direct synthesis, or via ligand exchange.

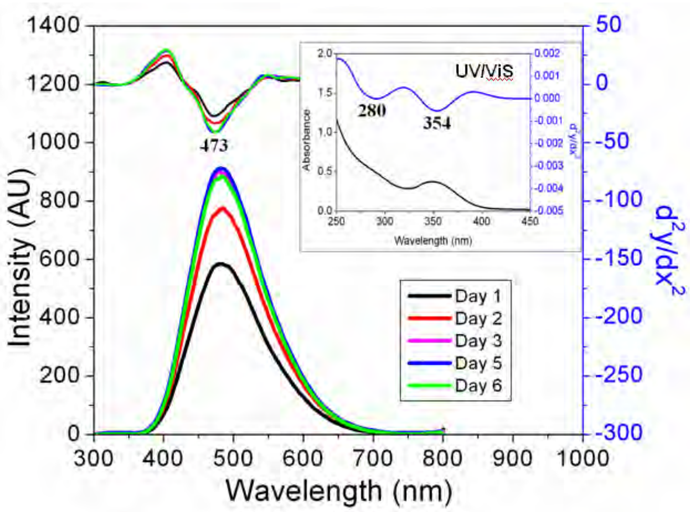

Figure 2. Synthesis of **6G**-PAMOH CdS QDs in **methanol** solution. The growth of the nanoparticles was monitored using fluorescence, UV/VIS absorption (insert) and second derivative spectra.

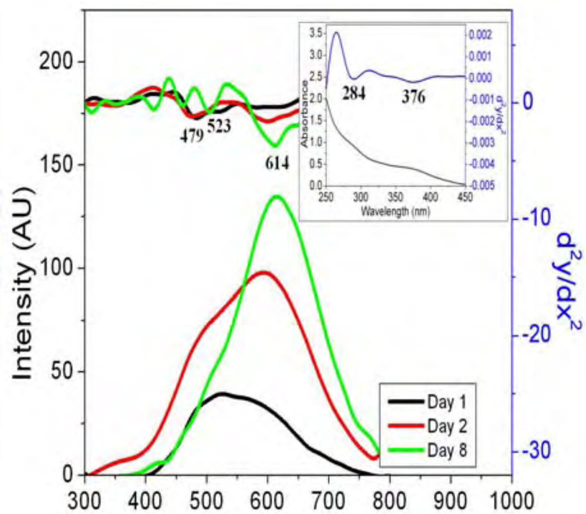

Figure 3. Synthesis of **6G**-PAMOH CdS QDs in ultrapure, 18.2 MΩ water. The growth of the QDs was monitored using fluorescence, UV/VIS absorption (insert) and second derivative spectra.

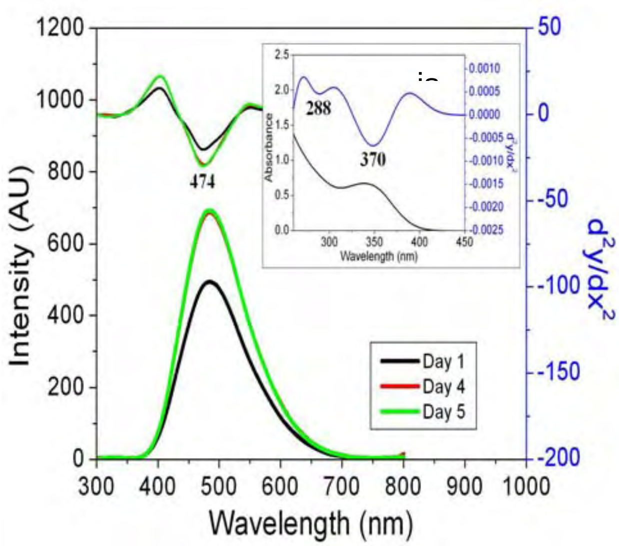

Figure 4. Synthesis of **5G**-PAMOH CdS QDs in **methanol** at room temperature. The growth of the QDs was monitored using fluorescence, UV/VIS absorption (insert) and second derivative spectra.

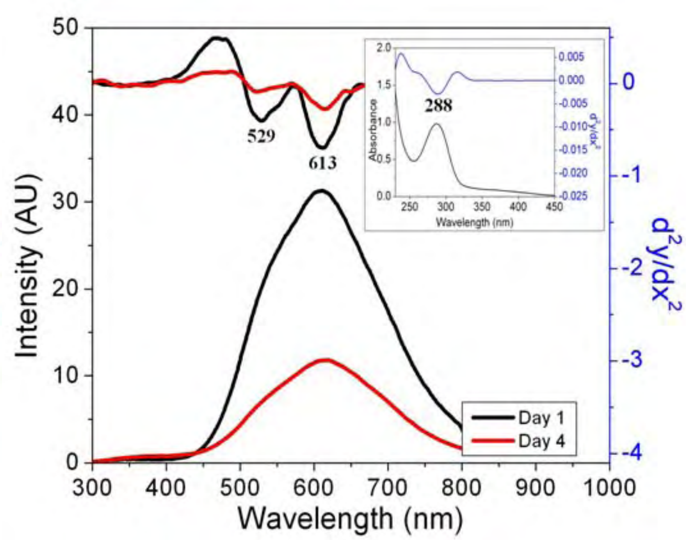

Figure 5. Synthesis of **5G**-PAMOH CdS QDs in ultrapure 18.2 MΩ **water** at room temperature. The growth of the QDs was monitored using fluorescence, UV/VIS absorption (insert) and second derivative spectra.

The data shown in Figures 2-5 was obtained as a result of hundreds of experiments in which the reaction conditions, such as the concentration of the dendrimers, sulfide and cadmium ion concentrations, the dendrimer/ion concentration ratio, addition times, reaction times, rates of addition, and pH, were optimized. The reactions were carried out in degassed media, under argon atmosphere, at room temperature.

Comparison of 4^{th}, 5^{th}, and 6^{th} generation PAMOH dendrimers revealed that the 5^{th} and 6^{th} generation dendrimers formed more intensely fluorescent CdS QDs. Moreover, the CdS QDs protected by the higher generation PAMAM dendrimers were significantly more stable than those protected with 4^{th} generation PAMOH dendrimer, therefore efforts were focused on the synthesis and characterization of 5^{th} and 6^{th} generation nanocomposites (Figure 6).

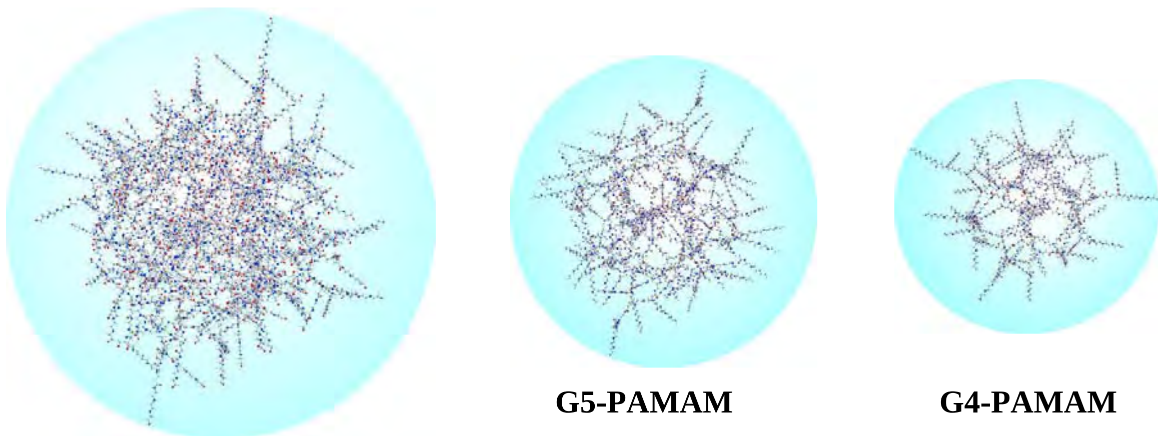

G6-PAMAM

- **MW: 69,351.62**
- **256 terminal groups**
- **254 tertiary amines**

G5-PAMAM

- **MW: 34,491.60**
- **128 terminal groups**
- **126 tertiary amines**

G4-PAMAM

- **MW: 17,061.58**
- **64 terminal groups**
- **62 tertiary amines**

Figure 6. 3D structures and other molecular characteristics of the G6-, G5-, and G4-PAMAM dendrimers.

Biological and medical imaging, targeted drug delivery, and diagnostic applications all require optically stable QDs soluble in aqueous media. However, synthesis of colloidally and optically stable water-dispersible QDs remains a challenge, therefore only a few recent studies have reported successful preparation of biocompatible QDs.[2-6] These syntheses employed amphiphilic polymers to stabilize CdSe/ZnS QDs, or phospholipids micelles to stabilize Si QDs, or used ligand exchange followed by capping with poly(acrylic acid) to stabilize iron oxide and TiO_2 nanoparticles in water. The drawbacks using the above methodologies are numerous. They include lower fluorescence quantum yields, emission maxima in the visible range resulting in poor tissue penetration, incomplete ligand exchange or decomposition during ligand exchange, and complex, tedious procedures. The work described here demonstrates that direct synthesis of QDs in water is feasible by synthesizing CdS quantum dots in hydroxyl-terminated dendrimers.

In the course of the synthesis of biocompatible QDs, we realized that gentle curing at 50 ^{o}C for 2 hours, or 70 ^{o}C for 1 hour can speed up the process that normally took several days at room temperature. Thus, when the synthesis was carried out in water at rt, the initially observed emission maxima of the freshly synthesized sample of G6-PAMAM encapsulated QDs (at 480/520 nm shifted to 650 nm with concomitant enhancement of intensity (Fig. 3, green curve) when the sample was cured an hour at 70 ^{o}C.

Other experiments showed that storage at room temperature over extended periods affected the fluorescence emission of the G6-PAMOH CdS QDs (Figure 7). The fluorescence intensity dropped and shifted to longer wavelengths (λ_{max}=650 nm), taking up to two weeks to stabilize at room temperature. This same red shift to 650 nm could be achieved faster, by heating the sample for 1 hour at 70 ^{o}C.

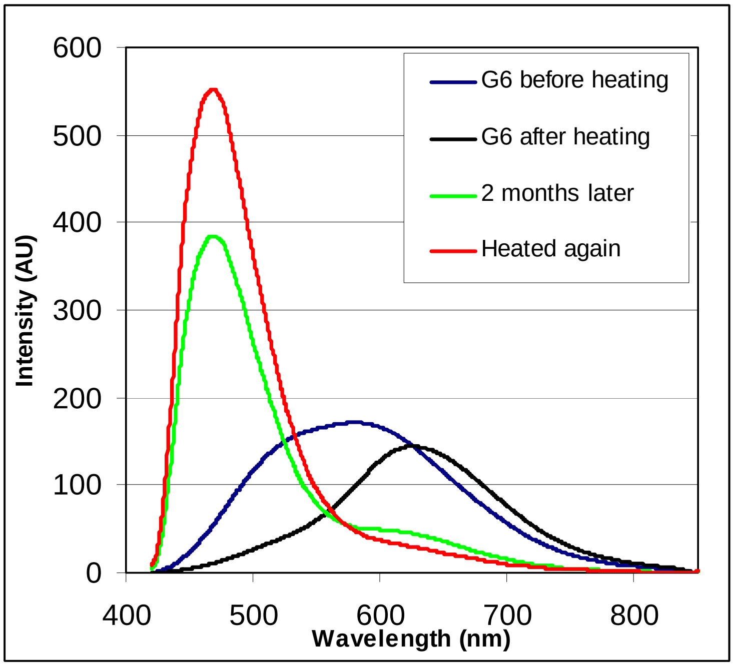

When the 650 nm emitter was stored in the dark for 2 months it slowly converted to a blue emitter (λ_{max}=470 nm). Heating to 70 ^{o}C completed the conversion of the red emitter into the blue emitter. Planned HRTEM studies will help to elucidate the nature of these intriguing, interconvertible red/blue emitters.

Figure 7. Changes in the emission spectrum of 6G-PAMAM CdS QDs.

The biocompatible synthesis of CdS QDs in water resulted in large Stokes shifts, and afforded QDs emitting close to the NIR range. However, to achieve better tissue penetration, the synthesis of dendrimer-encapsulated PbS QDs had to be undertaken. Based on the experience with synthesis of the dendrimerized CdS QDs, two types of syntheses were followed to obtain the target compounds: (1) Synthesis via ligand exchange, and (2) Direct synthesis (Figure 8).

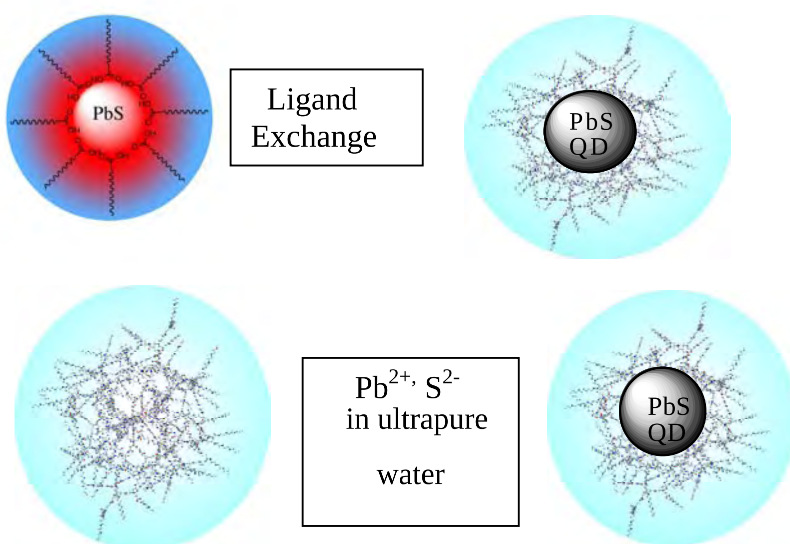

Figure 8. Synthetic routes to dendrimerized 6G-PAMAM PbS QDs.

In the ligand exchange process, the weaker carboxyl ligands of the oleic acid in the inverted micelle structure are exchanged for the stronger amine ligands within the dendrimer. The exchange reaction was monitored via transmission electron microscopy (TEM). Figure 9 shows the PbS QDs within the inverted micelles, and Figure 10, shows the PbS QDs encapsulated within 6G-PAMAM dendrimers.

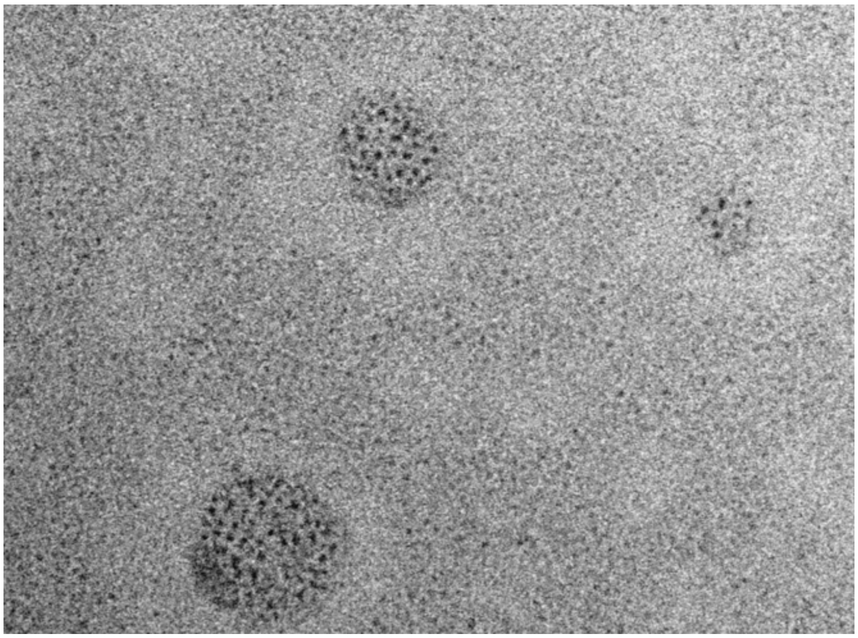

Figure 9. TEM images of PbS QDs in inverted micelles of oleic acid. Before ligand exchange

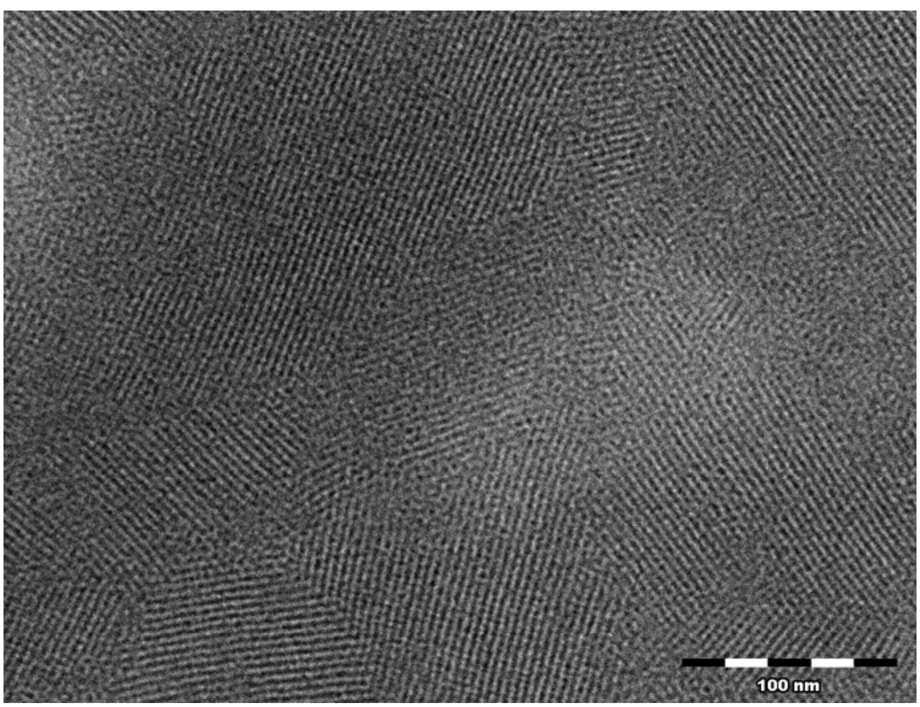

Figure 10. TEM image of PbS QDs in 6G-PAMAM dendrimer matrix after ligand exchange. The branches of the dendrimer were optimized for ligand exchange, and the surface of the dendrimers were optimized for facilitating self-assembly.

The size of PbS QDs is 2.9 nm, and they have the typical hexagonal wurzite structure.

Specific Aim 2. Synthesize polyazamacrocyclic chemokine mimics with linkers for conjugation

Task 3. Synthesize polyazamacrocyclic chemokine mimic, VBN-19, with a three carbon linker using [2+2] macrocyclyzation reaction.

In order to better assess the potential of the VBN-chemokine mimics, instead of a single VBN-19 compound, three analogs VBN-18, VBN-19R, and VBN-25 were prepared according to previously established synthetic routes. All three analogs were then conjugated, and were also submitted to the following toxicity studies in collaborative arrangements:

Specific Aim 3. Derivatize the periphery of the dendrimer QDs with multiple copies of the polyazamacrocyclic chemokine mimic VBN-19 and study their spectroscopic characteristics.

Task 4. Derivatize the periphery of the G5-PAMAM–dendrimeer encapsulated QD with multiple copies of the chemokine mimic VBN-19 (8-10 months)

Task 5. Measure the absorption and fluorescence spectra of 5G-PAMAM dendrimer encapsulated QDs conjugated with multiple copiesof polyazamacrocyclic chemokine mimic VBN-19 (8-10 Months).

Since the toxicity data as well as the chemokine activity pointed to a derivative of VBN-19, VBN-19R as the more suitable compound for further testing, attempts were made to conjugate VBN-19R to the 6G-PAMAM PbS QDs' surface. According to the reaction's stoichiometry, at least 4-5 units of VBN-19R should have been attached per surface. However, it is very difficult to estimate the exact amount within the large G6- polymer of MW= 69,351 without measuring the 800 or 900 MHz NMR spectra of the conjugate. A better approach will be the synthesis of series with different stoichiometries and determination of their chemokine activity in collaboration studies. The active compounds will then be selected for full structural elucidation.

Specific Aim 4. Study the absorption and fluorescence spectra, fluorescence kinetics, and emission anisotropy of the synthesized nanocomposites, provide feedback for synthesis, and test their efficacy through imaging experiments.

Task 6. Measure the absorption and fluorescence spectra of 5G-PAMAM-dendrimer encapsulated QDs and conjugates. Measure fluorescence lifetime, emission anisotropy. Provide feedback for optimizing syntheses. (1-11 months)

Absorption and Emission Spectra

The absorption spectra of the synthesized QD-dendrimer hybrid nanocomposites were measured at room temperature using a UV-visible-NIR spectrophotometer (Perkin-Elmer Lambda-9). The fluorescence spectra in the 400-750 nm spectral range were measured using a fluorometer (Perkin-Elmer LS-50). These spectra provided guidance for the synthesis process, as has been outlined in the *Specific Aim 1 Section*.

Figure 2, Figure 3, Figure 4, and Figure 5 show the room-temperature optical emission spectra and absorption spectra (insets) of CdS QD-6G PAMOH in methanol, CdS QD-6G PAMOH in water, CdS QD-5G PAMOH in methanol, and CdS QD-5G PAMOH in water, respectively. Also shown in the insets of these figures are the respective second derivative spectra.

The absorption spectra of all four nanocomposites are characterized by strong blue shift of the absorption band edge compared to that of the bulk CdS (512 nm). This blue shift is a consequence of quantum confinement effect and provides an indication that the nanocomposites are being formed, and can be used to obtain estimates of the size of the CdS-QDs being formed. Table 1 summarizes the spectral position of the first absorption peak of the nanocomposites.

Table I. Spectroscopic properties of the nanocomposites

Nanocomposite	First Absorption peak (nm)	Emission peak (nm)	Emission Range (nm)
CdS QD-6G PAMOH in methanol	354	473	400 -700
CdS QD-6G PAMOH in water	376	614	400-750
CdS QD-5G PAMOH in methanol	370	474	400-675
CdS QD-5G PAMOH in water	288	613	450 -850

All four nanocomposites exhibit broadband fluorescence. As shown in Table I, the nanocomposites synthesized in water had their emission peaks much further red shifted (614 nm, 613 nm) than those synthesized in methanol (473 nm, 474 nm). Nanocomposites in methanol solution fluoresced more strongly than those in water. The ability to synthesize the hybrid nanocomposites in water, and the substantial red shift of fluorescence of the nanocmposites thus synthesized are among the important achievements of this work, because biomedical applications require contrast agents or drug delivery agents to be optically stable in acqueous media.

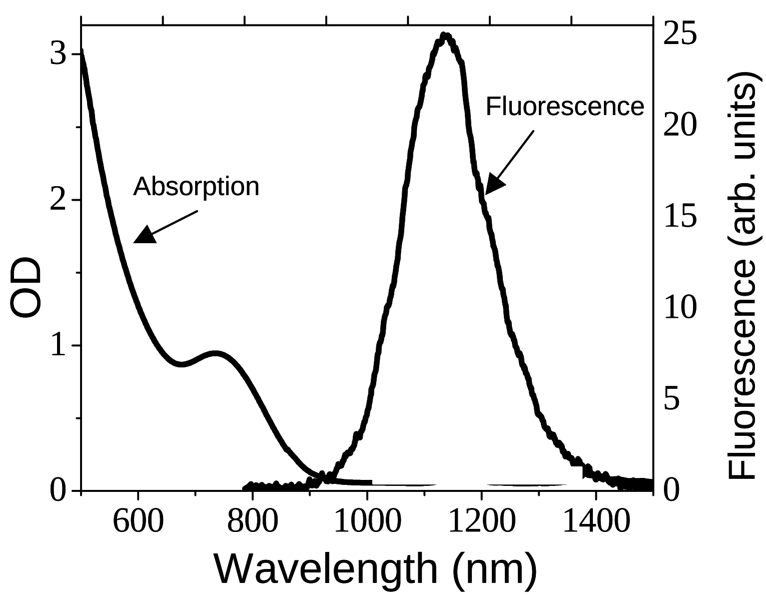

Figure 11. Optical absorption (left) and fluorescence (right) spectra of PbS QD- 6G PAMAM. The sample was contained in a 2-mm thick quartz cell.

To obtain nanocomposites those emit in the NIR (NIR radiation has higher penetration into biological tissues) nanocomposites based on PbS QDs encapsulated in G6-PAMAM dendrimer were synthesized. The absorption and emission spectra of the PbS QD-G6-PAMAM nanocomposite is shown in Fig. 11. The fluorescence was excited using the 698-nm output of a diode laser, dispersing the fluorescence through a monochromator and sensing the dispersed fluorescence using a PbS-photodetector.

The first absorption peak (band-edge absorption) appears at 750 nm, which is substantially blue shifted compared to that of the bulk PbS (3.38 μm). This blue shift is again a consequence of the quantum confinement effect, as the QD of size is assessed to be ~3 nm from TEM measurements. The emission spectrum spans the 800-1200 nm range with a peak at 940 nm.

Fluorescence Lifetime

The time evolution of nanocomposite fluorescence was measured by exciting into the absorption band using ultrashort light pulses of appropriate wavelength, and monitoring the resulting fluorescence in the time domain using a fast photodetector. The fluorescence from CdS-QD based nanocomposites had a faster component and a slower component, similar to the behavior observed in the CdS:DAB nanocomposite.[7] The samples were excited using 100-fs, 375-nm frequency doubled output of a Ti:sapphire laser and amplifier system.[8] The fast component was measured using a streak camera (Hamamatsu Model C5680) with a typical temporal resolution of 6 ps. The time evolution of the slower component was measured using a photomultiplier tube, and analyzing the fluorescence temporal profile using a 50-ohm terminated digital oscilloscope. The latter arrangement was used to measure the fluorescence dynamics of the PbS QD-G6-PAMAM nanocomposite with the exception of fluorescence being excited by the 750-nm fundamental output of the Ti:sapphire laser system.

A fit to the initial part of the temporal profile assuming a relationship of the form

$$I(t) = I_1\, exp(-t/\tau_1) + I_s(t), \qquad (1)$$

provided the decay time for the fast component. In Eq.(1) I_1 is the peak value, and $I_s(t)$ is the quasi-steady (on the picosecond time scale) value of the fluorescence intensity, and τ_1 is the decay time of the faster component. The long component of the fluorescence temporal profile could be fitted to a single exponential to extract the decay time.

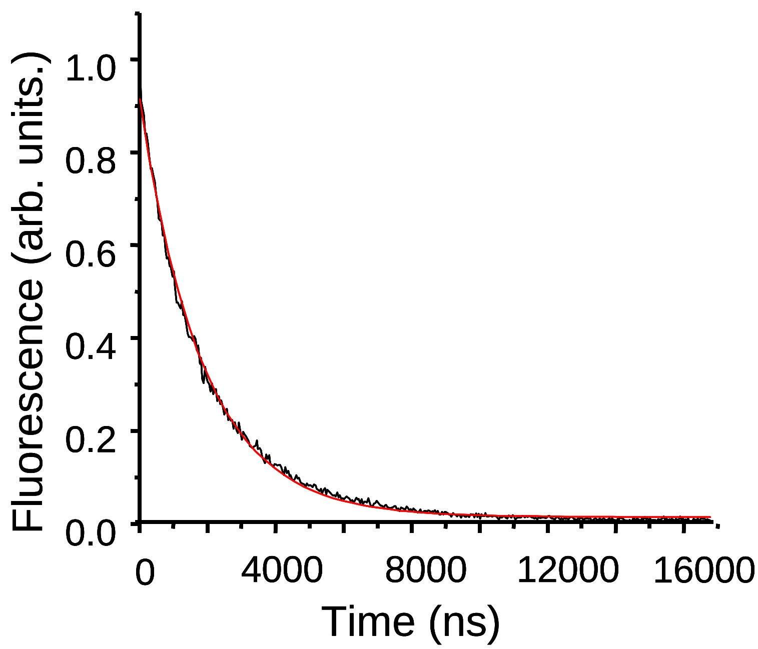

Figure 12. Room temperature fluorescence decay of PbS QDs in inverted micelles of oleic acid. The red line is a fit to the experimental data represented by the black line.

The PbS QD exhibited a single exponential decay with a longer lifetime of 1845 ns (Fig. 12.) However, the PbS QD-G6-PAMAM nanocomposite fluorescence lifetime was shorter, 1396 ns. We attribute this shortening of lifetime to more nonradiative decay channels that become available because of incorporation in the PAMAM dendrimer matrix.

Table II. Fluorescence lifetimes of the nanocomposites

Nanocomposite	Lifetime, τ_1 (ps)	Lifetime, τ_2 (ns)
CdS QD-6G PAMOH in water	322 ± 6	500 ± 12
CdS QD-5G PAMOH in water	457 ± 8	440 ± 8
PbS QD-G6-PAMAM in water		1396 ± 11

Table II presents the fluorescence decay times of the CdS-QD based nancomposites synthesized in water, and of PbS QD-G6-PAMAM in water.

Task 7. Carry out optical imaging experiments using Intralipid-10% suspension in water as the breast tissue-simulating specimen to test the efficacy of the nanocomposites. (9-12 months)

The potential of the nanocomposites as fluorescence contrast agent for imaging applications was tested in an imaging experiment. A suspension of Intralipid-10% in water, and a slab of chicken breast tissue were used as the breast tissue simulating scattering media.

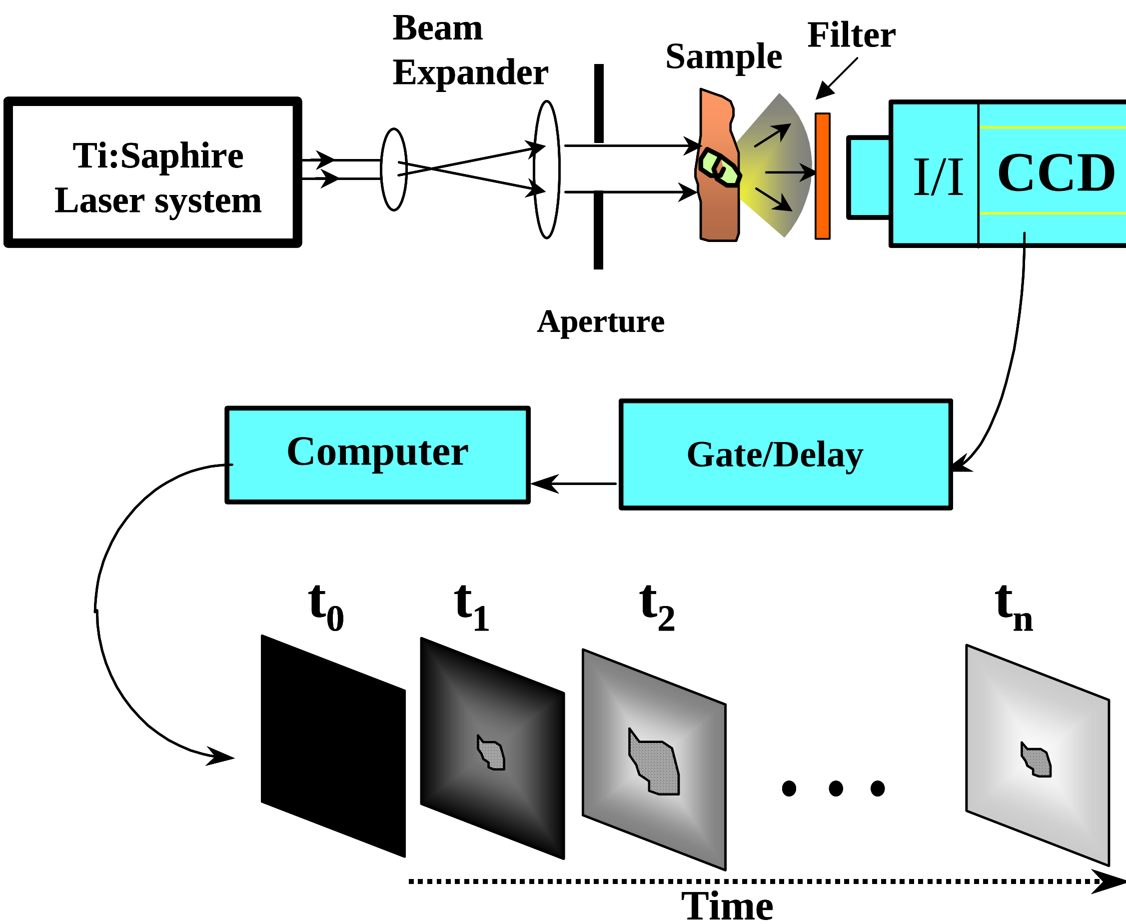

Fig. 13. A schematic diagram of the experimental arrangement for fluorescence optical imaging.

The *imaging* experimental arrangement, shown schematically in Fig. 13, used 120-fs duration, 1-kHz repetition-rate, 800-nm light pulses form a Ti-sapphire laser and amplifier system for probing the sample, and an ultrafast gated intensified camera system (UGICS) for recording 2-*D* images.[9] The UGICS is a compact gated image intensifier unit fiber-optically coupled to a charged-coupled device (CCD) camera. It provides an electronic gate pulse whose full-width-at-half-maximum duration can be adjusted to a minimum of 80-ps, and the position of the time gate could be varied over a 20 ns range with a step size of 25 ps (or some integral multiple of it). The signal recorded by the UGICS at a particular gate position, t_i is a two-dimensional (2-*D*) image, that is, a 2-*D* intensity distribution $I(x, y, t_i)$ formed by the convolution of the transmitted light pulse with the gate pulse centered on the gate position.

The Intralipid-10% suspension in water (transport length 2.3 mm at 800 nm) was held in a 10 cm X 10 cm X 4 cm transparent plastic container. The target was the PbS QD-G6-PAMAM nanocomposite in water contained in a 5-mm outer diameter (2 mm inner diameter) tube. The sample was placed in the middle of the 4-cm path length of the container. The diffuse fluorescence from the target was collected by a camera lens through optical filters that blocked the 800-nm pump beam, but transmitted a narrow band of fluorescence around 832 nm. The fluorescent target appears as a brighter region on a darker background. The corresponding spatial intensity profile shows a peak in the target position. Time-resolved images were recorded at different intervals within the 20-ns range, and indicated that not only fluorescence imaging, but fluorescence lifetime imaging may also be accomplished with this QD-based contrast agent.

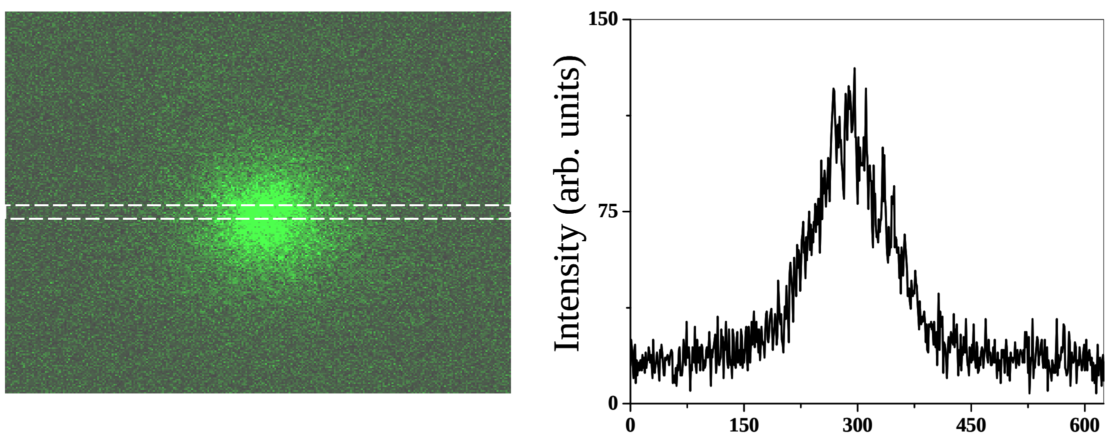

Fig. 14. Time-gated two-dimensional fluorescence image (left) of a small piece of chicken tissue impregnated with PbS-based nanocomposite solution placed within a slab of chicken tissue described in the text. Spatial Intensity profile (right) of the image along the region enclosed by the white dashed line.

To simulate a more realistic target we soaked a ~2mm X 2mm X 2mm piece of chicken tissue with the nanocomposite solution and placed it inside a 40 mm X 40 mm X 10 mm chicken tissue block. Imaging measurement was carried out through the 10 mm path length. Again a brighter image of the fluorescent target in a darker background was obtained. The result of imaging measurement is shown in Fig. 14.

Specific Aim 5. Test the effect of chemokine mimics on breast cancer cells in collaborative studies

Task 8. With our collaborators in the Biology Department at CCNY, and at Memorial Sloan Kettering Cancer Center test the effect of the chemokine mimic nanocomposite on established breast cancer cells. (11-12 months)

Toxicity studies:

- All three chemokine mimics, VBN-18, VBN-19R, and VBN-25, were tested for toxicity by Dr. Mary L. Alpaugh (Department of Biology at CCNY) using the cell line MDA MB 468, human Black, breast epithelial derived from an adenocarcinoma. Cell line is tumorigenic in immune-compromised mice (from ATCC). Stock solutions of 8.2×10^{-3} M of VBN-18, 7.8×10^{-3} M (in ethanol), of VBN-19R (in ethanol), and 4.07×10^{-3} M of VBN-25 (in water) were prepared and appropriate dilutions were made to determine toxicity. It was determined that none of these chemokine mimics was toxic to the cells in the concentration range of 5-100 μg/mL.
- Toxicity against H9 T cells, and chemokine activity in pre and post-infection assays was determined by Dr. Robert R. Finberg laboratories at Harvard Medical School & Dana Farber Cancer Institute. None of the three VBN-chemokine mimics was toxic to H9 T cell lines up to 50 μg/mL, and they showed chemokine activity at or close to 25 μg/mL (VBN-19R).

These studies are highly encouraging because none of the three chemokine mimics tested displayed toxicity, and a derivative of VBN-19 (VBN-19R) showed significant CXCR4 chemokine activity.

Task 9. Develop a hypothesis-based research proposal based on the data accumulated during the project for supporting this important line of work in the future. (11-12 months)

We are developing a proposal based on the work accomplished in the current Concept Award, and plan to submit it in the Idea Award category in next year's BCRP solicitation. We also plan to seek support from National Institute of Health for this line of research.

6. KEY RESEARCH ACCOMPLISHMENTS

- Synthesis of multivalent, hybrid nanocomposites has been accomplished in water. The method is the first straightforward bench top synthesis of water-soluble, biocompatible quantum dot nanocomposites at room temperature. It represents a general approach to the synthesis of hybrid inorganic/organic nanocomposites in aqueous media thereby greatly extending their possible applications. The dendrimer matrix employed here to stabilize the nanoparticles in water also provide a multivalent platform for interface with biomolecules at the dendrimer surface. This interface is critical for the synthesis of QD bioconjugates designed to prevent breast cancer micrometastases.
- A gentle method was established to further stabilize the nanocomposites synthesized in water, and to concomitantly and significantly shift their fluorescence emission to the desired NIR range highly desirable for *in vivo* imaging.
- The synthesis of NIR emitting, dendrimerized PbS QDs was accomplished using both fifth and sixth generation PAMAM dendrimers for encapsulation and self-assembly, yielding hexagonal wurzite-type structures.
- The CdS-based water-soluble nanocomposites emit in the red and PbS-based nanocomposites emit in the near-infrared, and are suitable for application as contrast agents in biomedical imaging.
- Imaging experiments involving these fluorophores as targets within breast tissue simulating media indicate their potential as contrast agents.

- The synthesis of three chemokine mimics VBN-18, VBN-19R, and VBN-25 (instead of the proposed single one, VBN-19) was accomplished. This allows a fuller evaluation of the nanocomposites' toxicity/chemokine potential.
- None of the three synthetic VBN-chemokine mimics was toxic to MDA MB 468 breast cancer cell lines at concentrations at which chemokine mimic activity was observed in the pre- and post-infection assays in the Harvard pre- and post-infection experiments.
- Their biocompatibility, their multivalency, their optical properties, and the fact that the three lead nanocomposites obtained to date are not toxic to breast cancer cells, and that they act as chemokine mimics, indicate their high potential in preventing micrometastases.

7. REPORTABLE OUTCOMES

Presentation and Proceedings

V. Balogh-Nair, A. Byro, F. Wang, R. Muthukattil, Y. F. Tse, H. Nguyen, B. B. Das, R. R. Alfano, and S. K. Gayen, "Synthesis and optical spectroscopic properties of multivalent and biocompatible hybrid cadmium sulfide-dendrimer nanocomposites." Poster P44-9 presented at the *Era of Hope* Department of Defense Breast Cancer Research Program Meeting, June 25-28, 2008, Baltimore, Maryland, and included in the meeting Proceedings, p. 310.

Articles

1. A. Byro, F. Wong, R. Muthukattil, V. Balogh-Nair, "Green Synthesis of Biocompatible, Dendrimer-encapsulated PbS QDs Using Self-assembly," to be submitted for publication in *ACS-NANO* (2008).
2. V. Balogh-Nair, A. Byro, F. Wang, R. Muthukattil, Y. F. Tse, H. Nguyen, B. B. Das, R. R. Alfano, and S. K. Gayen, "Optical spectroscopy of multivalent hybrid CdS-dendrimer and PbS-dendrimer nanocomposites." (In preparation)

8. CONCLUSION

The major goals and objectives of the proposed project were accomplished by the synthesis of NIR emitting dendrimer-encapsulated QDs to which synthetic chemokine mimics were attached via the dendrimers' surface. Optical Imaging experiments demonstrate the feasibility of using the nanocomposites as fluorescent contrast agents. In collaborative studies, it was established that the three VBN-compounds synthesized and tested were not toxic, and one of them (VBN-19R) displayed significant chemokine activity. These observations demonstrated the feasibility of the proposed hypothesis.

"***So What***"

The work accomplished in this project shows potential for developing nanocomposites that may help simultaneous detection and treatment of breast cancer. Much more work will be needed to realize that potential.

9. REFERENCES

1. L. Peng, C. Chen, C.R. Gonzalez, V. Balogh-Nair, Bioorganic Studies in AIDS: Synthetic Antifungals Against P. carinii Based on the Multivalency Concept, (2002) *Int. J. Mol. Sci.*, **3**, 1145-1161.
2. A.L.P. Cornacchio, N.D.. Jones, (2006) Thiolate-capped PbS nanocrystals in water: sensitivity to O2, pH, and concentration, an alternate pathway for crystal growth and a top-down synthesis, *J. Mater. Chem.*, **16**, 1171-1177.
3. Larson, D.R.; Zipfel, W.R.; Williams, R.M.; Clark, S.W.; Bruchez, M.P.; Wise, F.W.; Webb, W., Water-soluble quantum dots for multiphoton fluorescence imaging in vivo, *Science*, **2003**, 300, 1434-1436.
4. Han, H.; Cai, Y.; Liang, J.; Sheng, Z., Interaction between water-soluble CdSe quantum dots and gold nanoparticles studied by UV-Visible spectroscopy, *Analytical Sciences (The Japan Society for Analytical chemistry)* **2007**, 23, 651.
5. Zhang, T.; Ge, J.; Hu, Y.; Yin, Y., A general approach for transferring hydrophobic nanocrystals into water, *Nano Letters*, **2007**, 7, 10.1021/n1071928t.
6. Erogbogbo, F; Yong, K.-T.; Roy, I.; Xu, G.; Prasad, P.N.; Swihart, M.T., Biocompatible luminescent silicon quantum dots for imaging of cancer cells, *ACSNano*, **2008**, 10.1021/nn700319z.
7. S. K. Gayen, C. Gonzalez, V. Balogh-Nair, M. Brito, B. B. Das, G. Comanescu, X. C. Liang, A. H. Byro, David. L. V. Bauer, M. Alrubaiee, and R. R. Alfano, 'Optical Spectroscopy of a Hybrid CdS-Dendrimer Nanocomposite," *J. Opt. Soc. Am. B* 24, 3064 (2007).
8. Q. Fu, F. Seier, S. K. Gayen, and R. R. Alfano, "A high-average-power, kilohertz-repetition-rate, sub-100-fs Ti:sapphire amplifier system," *Opt. Lett.* **22**, 712 (1997).
9. W. Cai, S. K. Gayen, M. Xu, M. Zevallos, M. Alrubaiee, M. Lax, and R. R. Alfano, "Optical three-dimensional inverse image reconstruction of objects in turbid media from ultrafast time-sliced optical transmission measurements," *Appl. Opt.* **38**, 4237 (1999).

10. APPENDICES

Appendix 1. V. Balogh-Nair, A. Byro, F. Wang, R. Muthukattil, Y. F. Tse, H. Nguyen, B. B. Das, R. R. Alfano, and S. K. Gayen, "Synthesis and optical spectroscopic properties of multivalent and biocompatible hybrid cadmium sulfide-dendrimer nanocomposites." Poster P44-9 presented at the *Era of Hope* Department of Defense Breast Cancer Research Program Meeting, June 25-28, 2008, Baltimore, Maryland, and included in the meeting Proceedings, p. 310.

(*Please see the next page*.)

contrast agents for magnetic resonance imaging (MRI, with FeO in nanoshuttle) and computed tomography (CT) scanning. The objective of this work is to exploit the multimodal imaging properties and the programmable targeting capabilities of Au-phage nanoshuttles to improve the targeted treatment and detection of cancer. Here, we show the application of Au-phage nanoshuttles as the foundation for the development of in vivo and targeted NIR photo-therapies, MRI and CT scanning signal reporting, and NIR surface enhanced Raman scattering (NIR-SERS) detection. As part of this work, we have also begun to assess the toxicity of Au-phage nanoshuttles in the mouse, where no obvious effects associated with nanoshuttle administration were found to affect any of the parameters evaluated in our studies.

This work was supported by the U.S. Army Medical Research and Materiel Command under W81XWH-06-1-0775.

P44-8: FLUORESCENT CARBON DOTS AND BIOIMAGING APPLICATIONS

Ya-Ping Sun
Clemson University

Fluorescent semiconductor quantum dots have generated much excitement for a wide variety of promising applications, especially those in biology and medicine. For both in vitro and in vivo uses, however, the known toxicity and potential environmental hazard associated with many of these materials may represent serious limitations. Therefore, the search for benign nanomaterials of similar optical properties continues. For quantum-sized silicon, the discovery of Brus and coworkers on the strong luminescence in surface-oxidized nanocrystals has attracted extensive investigations of silicon nanoparticles and nanowires. We have discovered that small carbon nanoparticles (preferably less than 10 nm) can be made highly photoactive upon simple surface passivation, exhibiting strong photoluminescence in both solution and solid-state and with either one- or two-photon excitation. These luminescent carbon nanoparticles ("carbon dots") may find applications alternative to or beyond those of traditional semiconductor quantum dots. For example, they may be derivatized to recognize and bind to biologically active species. Some representative experimental results will be presented, along with discussion on the technology in breast cancer research and imaging applications.

This work was supported by the U.S. Army Medical Research and Materiel Command under W81XWH-06-1-0656.

P44-9: SYNTHESIS AND OPTICAL SPECTROSCOPIC PROPERTIES OF MULTIVALENT AND BIOCOMPATIBLE HYBRID CADMIUM SULFIDE-DENDRIMER NANOCOMPOSITES

Valeria Balogh-Nair, Andrew Byro, Flory Wang, Ronex Muthukattil, Yiu Fat Tse, Hanh Nguyen, Bidyut Baran Das, Robert R. Alfano, and Swapan Kumar Gayen
City University of New York

Background and Objectives: Hybrid nanocomposites of semiconductor quantum dots (QDs) and organic dendrimers are of great interest because their small size, emission tunability, superior photostability and longer luminescence decay times, in comparison with dyes, turn them into promising materials for applications such as contrast agents for biomedical imaging and bioconjugates for nanomedicine. A major challenge is to obtain water soluble biocompatible QDs suitable for the synthesis of bioconjugates designed to prevent breast cancer micrometastases and/or to be used in biomedical imaging application. Here we report on the synthesis of water-soluble nanocomposites of cadmium sulfide (CdS) QDs in polyamidoamine (PAMAM)-amidoethylethanolamine type dendrimer and the characterization of the QDs using absorption and fluorescence spectroscopies.

Brief Description of Methodologies: Cadmium sulfide QDs were synthesized using sixth, fifth, and fourth generation dendrimers (G6-PAMOH, G5-PAMOH, and G4-PAMOH) as nanoreactors. Stock solutions of Cd^{2+} and S^{2-} ion precursors were injected into stirred solutions of the dendrimers in ultrapure degassed water, under argon atmosphere and the mixtures were stirred until maximum growth of the nanoparticles was achieved. Alternatively, QDs prepared in methanol solution could be subsequently transferred into water. The growth of the particles was monitored using ultraviolet-visible absorption and fluorescence spectroscopy. The excitation and emission spectra, as well as their second derivatives, were also measured to establish the emission characteristics of the QDs. The time evolution of fluorescence was measured exciting the samples using the second harmonic radiation from a femtosecond Ti:sapphire laser generating 100-fs pulses at 82 MHz repetition rate. A streak camera measured the time evolution of fluorescence.

Results: All three generations of dendrimers formed fluorescent QDs in methanol solution, with emission maxima at around 470 nm, but only the two larger, fifth, and sixth generation dendrimers afforded nanoparticle synthesis in water. The fluorescence lifetimes measured in water yielded a decay time of 240 ps for the 6GPAMOH-CdS-QDs.

Conclusions: The method reported here is the first straightforward bench top synthesis of water soluble, biocompatible CdS quantum dots at room temperature. Moreover, the dendrimer matrix employed here to stabilize the nanoparticle in water also provides a multivalent platform for interface with biomolecules at the dendrimer's surface. This interface is critical for the synthesis of QD-bioconjugates designed to prevent breast cancer micrometastases.

This work was supported by the U.S. Army Medical Research and Materiel Command under W81XWH-06-1-0620.

P44-10: RADIOPAQUE, TUMOR-TARGETED NANOPARTICLES FOR IMPROVED MAMMOGRAPHIC DETECTION OF BREAST CANCER

Gregory Adams
Fox Chase Cancer Center

Background and Objectives: Despite the demonstrated utility of X-ray mammography for breast cancer screening, there is limited ability to image small or noncalcified lesions and to distinguish between benign and malignant microcalcifications. The sensitivity and specificity of mammography could be greatly improved if the X-ray attenuation of breast cancer tissue could be enhanced selectively using tumor-specific antibodies labeled with gold nanoparticles (AuNPs). After i.v. administration, these conjugates would clear rapidly from normal tissue but accumulate at breast tumors. The tumors could then be visualized by X-ray imaging due to the comparatively strong attenuation effect of the gold. Our objective was to perform preliminary studies towards developing gold nanoparticle immunoconjugates and determining their potential use in vivo.

Methods/Results: Initial studies were performed to determine if it would be possible to localize sufficient quantities of gold in tumors to alter the attenuation of X-rays in mammography studies. A 96 well acrylic cell culture plate was employed to represent an array of virtual "tumors." Each cylindrical well was then filled with a prescribed volume and concentration of AuNP suspension, thereby varying both attenuation length and tumor uptake. The entire apparatus was imaged by a conventional film mammography unit. Nanoparticle suspensions were prepared by diluting citrate-stabilized, 10 nm diameter AuNPs (Meliorum Technologies, Rochester, New York) in water. Ten concentrations ranging from 0.01 to 5 wt% gold were prepared in volumes ranging from 50 to 300 μL based on our calculations of expected tumor uptake (data not shown). Various imaging conditions (exposure time, peak kV, etc.) were examined. Quantitative examination by densitometry revealed a detectable increase in attenuation relative to baseline for higher concentrations of nanoparticles. These results suggest that the quantity of gold that must be deposited in a tumor to increase conspicuity should be attainable using conjugates between AuNPs and antibody fragments, particularly if repeat dosing were employed. Attempts to modify gold nanoparticles and render them reactive for conjugation to antibodies using a ligand substitution reaction in the presence of a stabilizing surfactant, e.g., Tween 20 resulted in irreversible aggregation and/or sedimentation of the AuNPs. This resulted in our need to explore alternative strategies. We developed a single-chain Fv (scFv) with C-terminal cys residues to facilitate attachment directly to AuNPs using known gold-thiol chemistry. In this scheme, no intermediate step of activating the AuNPs would be required. The gene encoding scFv-cys was successfully cloned and the scFv-cys protein was expressed, purified, and found to be fully functional using methods previously described [*Cancer Res.* 2001, 61:4750]. We are currently attempting to directly conjugate the scFv-cys to the AuNPs.

Conclusions: We have successfully demonstrated that AuNPs can enhance contrast on images obtained on a clinical mammography instrument. We encountered unanticipated difficulties in conjugating the C6.5 diabody to the AuNPs using our proposed methodology and were therefore forced to develop an alternate conjugation strategy, which we continue to evaluate. We are now in position to initiate comprehensive studies that will validate this approach for X-ray mammography contrast enhancement.

This work was supported by the U.S. Army Medical Research and Materiel Command under W81XWH-06-1-0591.

P44-11: TARGETING QUANTUM DOTS TO TUMORS USING ADENOVIRAL VECTORS

Maaike Everts, Jill M. Warren, Ryan G. Beam, and Vaibhav Saini
University of Alabama at Birmingham

Background/Objective: Despite advances in detection and treatment of cancer, development of novel therapies remains essential in the continuing battle against this disease: in this regard, nanotechnology holds great promise. For example, tumor imaging opportunities have expanded by the development of quantum dots (QDs) for fluorescence based detection, or magnetic nanoparticles for magnetic resonance imaging applications. However, for all these applications of metal nanoparticles, selective tumor targeting is crucial for successful clinical application. Considering the great progress made in targeting adenoviral (Ad) gene therapy vectors to tumors, we therefore aim to couple QDs with targeted Ad vectors to achieve specific, selective tumor accumulation. This combination of novel nanotechnology developments and gene therapy targeting strategies is expected to lead to the development of a unique methodology for cancer detection and treatment.